Structural Eng. / Earthquake Eng. Vol. 4. No. 1, 147s-154s. April 1987
Japan Society of Civil Engineers (Proc. of JSCE No. 380/I-7)

RESPONSE ANALYSIS OF BURIED PIPELINES CONSIDERING RISE OF GROUND WATER TABLE IN LIQUEFACTION PROCESSES

By Masaru KITAURA, Masakatsu MIYAJIMA** and Hiroshi SUZUKI****

Hybrid procedure is developed in order to analyze the behavior of buried pipelines in soil liquefaction processes. The procedure presented herein consists of a ground response evaluation using the finite element method and a pipe response analysis using the transfer matrix method. A rise of the ground water table induced by dissipation of excess pore water pressure is considered in the former evaluation. Numerical models show that the unsaturated layer around the pipelines liquefies due to the rise of the ground water table and accumulation of the excess pore water pressure. It is evident from the present study that the response characteristics of the buried pipelines change in the liquefaction process.

Keywords : buried pipeline, liquefaction, seismic response

1. INTRODUCTION

The 1983 Nipponkai-Chubu Earthquake damaged buried pipelines extensively. Much of these damages were caused in the area where sand boils erupted[1]. The results of the investigation of the earthquake damage revealed that a high damage ratio appeared in the area where the ground water table was 2m to 4m in depth[2]. The burial depths of pipelines are 1.2m to 1.5m in general. These facts suggest that the pipelines before the earthquake in the unsaturated sand layer were damaged due to soil liquefaction. It is, therefore, important to consider the rise of the ground water table in liquefaction processes when analyzing the response of pipelines. Based on these field investigation data, the factors of the pipe failures are considered as follows : (1) Transient large displacement of the surrounding ground of the pipelines when the sand layer under or near the pipelines is incompletely liquefied (the excess pore water pressure ratio is near to 1.0). (2) Buoyancy when the surrounding ground is completely liquefied (the excess pore water pressure ratio is 1.0). (3) Liquefaction-induced lateral spreading of the ground at a slope. The effects of the factors (1) and (2) are investigated in the present study.

Regarding the dissipation of the excess pore water pressure, two different approaches have been taken. One is based on the use of Terzaghi's consolidation equation[3]. The other is based on the Biot theory for the consolidation and the energy balance equation[4]. Both approaches, however, do not include the seepage of the pore water to unsaturated areas. On the other hand, many studies on the embedded pipe response have been performed[5)~7)]. Theoretical analysis on liquefaction-induced damage to pipelines, however, has been

* Member of JSCE, Dr. Eng., Professor, Department of Civil Engineering, Kanazawa University (2-40-20, Kodatsuno, Kanazawa, Ishikawa)
** Member of JSCE, M. Eng., Research Associate, ditto.
*** Member of JSCE, M. Eng., Japan National Railways.

rare.

The present paper proposes a hybrid procedure to analyze the behavior of the buried pipelines in the liquefaction process. This procedure consists of a ground response evaluation using the finite element method and a pipe response analysis using the transfer matrix method[8]. A rise of the ground water table induced by dissipation of excess pore water pressure was considered in the former evaluation. Numerical example shows that an unsaturated sand layer around the pipelines liquefies due to the rise of the ground water table and accumulation of the excess pore water pressure. Using the results of the ground response evaluation, a response simulation of the embedded pipelines is carried out.

2. DISSIPATION OF EXCESS PORE WATER PRESSURE CONSIDERING PERMEATION TO UNSATURATED AREAS

The equations of seepage in saturated-unsaturated porous media are given in Ref. 9). Applying the equation of motion concerning a system of solid, liquid and gaseous phases and neglecting the gaseous phase, the conservation of mass in the field of the fluid is then given by the following equation[9] :

$$\mathrm{div}\, q_r + n\frac{\partial S_r}{\partial t} + \kappa_w \theta \frac{\partial U_w}{\partial t} + S_r \frac{\partial \varepsilon}{\partial t} = 0 \quad \cdots\cdots (1)$$

in which q_r presents the relative specific volume discharge of liquid phase to solid phase, n=porosity, S_r =degree of saturation, θ=volumetric moisture content, κ_w=water compressibility, U_w=pore water pressure, ε=volumetric strain , t=time. The left hand side's first term represents the transfer of excess pore water and the second, third and fourth terms explain the storage due to the change of the degree of saturation, water compressibility and volume change of soil, respectively. Neglecting the compressibility of the pore water and soil respectively, the change in soil volume and applying Darcy's law to the systems, the equation of seepage in saturated-unsaturated porous media are :

$$\frac{\partial h_p}{\partial t} = \frac{1}{\alpha \gamma_w}\left\{\frac{\partial}{\partial x}\left(k_x \frac{\partial h}{\partial x}\right) + \frac{\partial}{\partial y}\left(k_y \frac{\partial h}{\partial y}\right) + \frac{\partial}{\partial z}\left(k_z \frac{\partial h}{\partial z}\right)\right\} \quad \cdots\cdots (2)$$

$$\frac{\partial h_p}{\partial t} = \frac{1}{c}\left\{\frac{\partial}{\partial x}\left(k_x^* \frac{\partial h}{\partial x}\right) + \frac{\partial}{\partial y}\left(k_y^* \frac{\partial h}{\partial y}\right) + \frac{\partial}{\partial z}\left(k_z^* \frac{\partial h}{\partial z}\right)\right\} \quad \cdots\cdots (3)$$

in which h=total head, h_p=pressure head, $k_{x,y,z}$=coefficients of permeability in the saturated region, $k^*_{x,y,z}$=coefficients of permeability in the unsaturated region , α=soil compressibility, c=specific moisture capacity, γ_w=unit weight of water. Subscripts x, y and z denote Cartesian coordinates. The specific moisture capacity and coefficient of permeability in the unsaturated region are indicated as follows by Brooks and Corey[10].

$$\frac{k^*}{k} = \left(\frac{P_b}{S}\right)^{3\lambda+2} \quad \cdots\cdots (4)$$

$$c \equiv \frac{\partial \theta}{\partial h_p} = \lambda(n-\theta_r)\frac{P_b^\lambda}{S^{\lambda+1}} \quad \cdots\cdots (5)$$

in which θ_r=volumetric moisture content in the state of constant water content. P_b=bubbling pressure, S=suction, λ=pore size distribution index.

3. ACCUMULATION OF EXCESS PORE WATER PRESSURE

The model of the pore water pressure generated during an earthquake proposed by Martin, Finn and Seed[11] is used in the present study. The rise of the pore water pressure Δu, caused in a cycle of shear strain during an undrained test is given by

$$\Delta u = \overline{E}_r \Delta \varepsilon_{vd} \quad \cdots\cdots (6)$$

in which $\overline{E}_r$ is the one dimensional rebound modulus of the sand at an effective stress σ'_v and $\Delta\varepsilon_{vd}$=the potential volumetric strain change associates with γ. The relationship between the total accumulated volumetric strain $\Delta\varepsilon_{vd}$ and the shear strain amplitude γ has been demonstrated by Martin, Finn and

Seed[11].

$$\Delta\varepsilon_{vd}=C_1(\gamma-C_2\varepsilon_{vd})+\frac{C_3\varepsilon_{vd}^2}{\gamma+C_4\varepsilon_{vd}} \quad (7)$$

For crystal silica sand with a relative density D_r=45%, C_1=0.80, C_2=0.79, C_3=0.45 and C_4=0.73 and $\Delta\varepsilon_{vd}$, ε_{vd}, γ expressed in percentages, the volume change at another relative density is obtained from

$$\Delta\varepsilon_{vd}|_{D_r=a}=\Delta\varepsilon_{vd}|_{D_r=45}\cdot R \quad (8)$$

$$R=0.0003(100-a)^2+0.062 \quad (9)$$

in which D_r indicates the relative density and $\Delta\varepsilon_{vd}|_{D_r=a}$ the volumetric strain change in case of a relative density of a %. The rebound modulus $\overline{E}_r$ at any effective stress level σ'_v is given by the next equation.

$$\overline{E}_r=\frac{(\sigma'_v)^{1-m}}{mk_2(\sigma'_{v0})^{n-m}} \quad (10)$$

in which σ'_{v0}=the initial effective stress, and m, n and k_2 are experimental constants. For the crystal silica sand at D_r=45 %, these values are given as follows: k_2=0.0025, m=0.43 and n=0.62.

4. NON-LINEAR MODEL OF GROUND

The variation of the shear modulus due to the magnitude of strain is described by Hardin and Drnevich[12].

$$G=G_0\frac{\gamma_m}{\gamma_m+\gamma} \quad (11)$$

in which G_0=initial shear modulus, γ=shear stress and γ_m=reference strain ($\gamma_m=\tau_m/G_0$, γ_m=shear stress at failure). In the present study a hyperbolic stress-strain hysteresis curve is not used, but a simplified linear stress-strain relation because the shear modulus is constant during one cycle of shear stress and then the change of the excess pore water pressure is evaluated and the shear modulus is computed by substituting Eqs. (12) and (13) into Eq. (11).

$$G_0=(G_0)_{\sigma_{v0}}\left(\frac{\sigma'_v}{\sigma'_{v0}}\right)^{\frac{1}{2}} \quad (12)$$

$$\gamma_m=(\gamma_m)_{\sigma_{v0}}\left(\frac{\sigma'_v}{\sigma'_{v0}}\right)^{\frac{1}{2}} \quad (13)$$

in which σ'_{v0}=initial effective confining stress, σ'_v=effective confining stress at any cycle of shear stress. These equations mean that the shear modulus and reference strain are proportional to the root of the change ratio of the vertical confining stress[13].

Concerning damping ratios, the internal damping ratio h_η and the hysteretic damping ratio h_h are considered in this analysis. The hysteretic damping ratio is presented as follows, using the Hardin and Drnevich model.

$$h_h=h_{\max}\frac{\gamma}{\gamma_m+\gamma} \quad (14)$$

in which $h_{\max}$ is maximum value of the hysteretic damping ratio. γ_m is calculated by Eq. (13). The internal damping ratio h_η is given by

$$h_\eta=0.0002\,V_s+0.017=0.0002\sqrt{\frac{G}{\rho}}+0.017 \quad (15)$$

in which V_s=velocity of the shear wave (m/s), ρ=density of the ground[14]. G is shear modulus calculated by Eq. (11). In order to control the stability of the calculation, it is assumed that the shear modulus is not less 1% of the initial value[15].

5. PROCEDURE OF COMPUTING RESPONSE OF GROUND AND PIPELINE

Fig. 1 shows the flow chart of the response analysis presented herein. The response analysis of the ground is performed using the finite element method. The procedure of evaluating generation and dissipation of the pore water pressure is as follows:

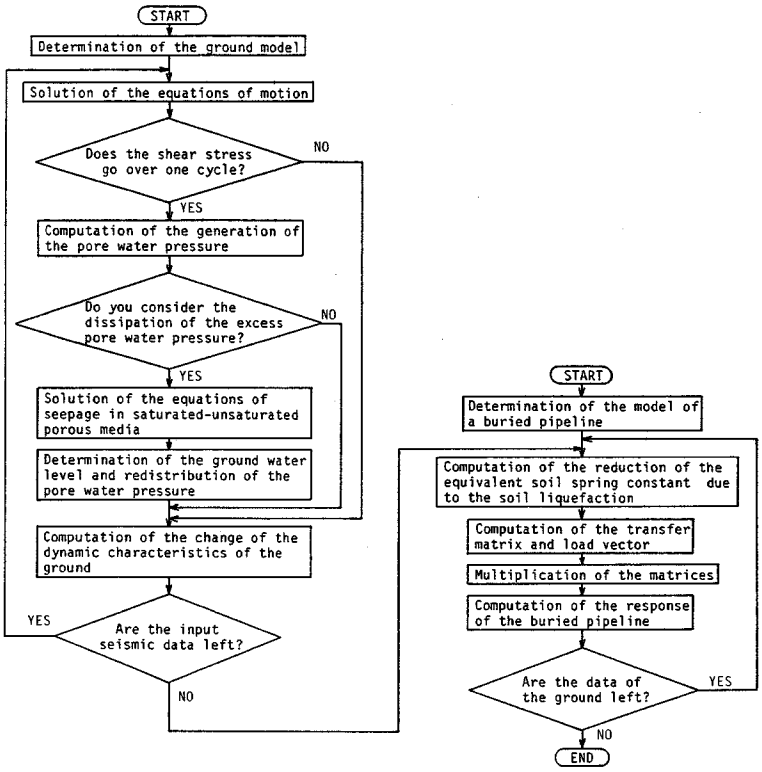

Fig. 1 Simulation flow chart.

1. Compute generation of the pore water pressure by means of the equations by Martin, Finn and Seed.
2. Evaluate dissipation of the pore water pressure by using the equations of seepage in saturated-unsaturated porous media (Eqs. (2) and (3)).
3. Determine the pore water pressure at any depth combining 1. and 2.
4. Derermine the ground water level. The depth where the pore water pressure is zero is the ground water level.
5. Based on the ground water level, determine the distribution of the excess pore water pressure at the respective time step.

This process is repeated at every one cycle of shear strain.

This response of the buried pipe is computed employing the modified transfer matrix method improving round off errors presented by Nakamura[16]. A pipeline is modeled as a series of segmented Winkler beams connected longitudinally by joints with springs for both axial and bending motions. Equivalent soil spring constants in liquefaction process are evaluated using the following empirical equation presented by Yoshida and Uematsu[17].

$$r=2.81+528.1/(100\cdot j-291.1) \quad \cdots\cdots (16)$$

in which r=reduction rate of the reaction force of sand ground and j=excess pore water pressure ratio.

6. NUMERICAL EXAMPLES

The sand deposit shown in Table 1 and Fig. 2 was analyzed employing the method presented in the previous chapter. The base rock motion consists of the first 30 seconds of the Taft E-W component, 1952, scaled at a maximum acceleration of 40gal. Fig. 3 shows the time history of the excess pore water pressure at the 4th sand layer. The results of the different methods are also in this figure. The excess pore water

Table 1 Physical properties of model ground I.

Depth (m)	Layer number	Unit weight (tf/m^3)	Initial effective stress (kgf/cm^2)	Initial shear modulus (kgf/cm^2)	Maximum value of damping ratio	Relative density (%)	Coefficient of permeability (cm/sec)	Poisson ratio	Reference shear strain
1.0	1	1.3	0.06	690	0.20	42.1	1.0×10^{-2}	0.4	4.2×10^{-4}
2.0	2	1.3	0.19	520	0.20	42.1	1.0×10^{-2}	0.4	4.2×10^{-4}
3.5	3	1.8	0.31	460	0.20	42.1	1.0×10^{-2}	0.4	4.2×10^{-4}
5.0	4	1.8	0.43	460	0.20	52.9	1.0×10^{-2}	0.4	4.2×10^{-4}
6.5	5	1.9	0.55	1200	0.20	47.1	1.0×10^{-2}	0.4	4.2×10^{-4}
8.0	6	1.9	0.68	1500	0.20	39.4	1.0×10^{-2}	0.4	4.2×10^{-4}
10.0	7	1.9	0.84	1500	0.20	40.8	1.0×10^{-2}	0.4	4.2×10^{-4}
12.0	8	1.9	1.02	1500	0.20	80.0	1.0×10^{-2}	0.4	4.2×10^{-4}
14.0	9	1.9	1.20	1500	0.20	80.0	1.0×10^{-2}	0.4	4.2×10^{-4}
18.0	10	2.0	1.48	3200	0.25	80.0	1.0×10^{-2}	0.4	4.2×10^{-4}
20.0	11	2.1	1.78	4300	0.25	80.0	1.0×10^{-2}	0.4	4.2×10^{-4}
24.0	12	2.1	2.11	4300	0.25	80.0	1.0×10^{-2}	0.4	4.2×10^{-4}
27.0	13	2.1	2.48	4800	0.25	80.0	1.0×10^{-2}	0.4	4.2×10^{-4}
30.0	14	2.1	2.81	6400	0.25	80.0	1.0×10^{-2}	0.4	4.2×10^{-4}

($1tf/m^3 = 9.8kN/m^3$, $1kgf/cm^2 = 98kPa$)

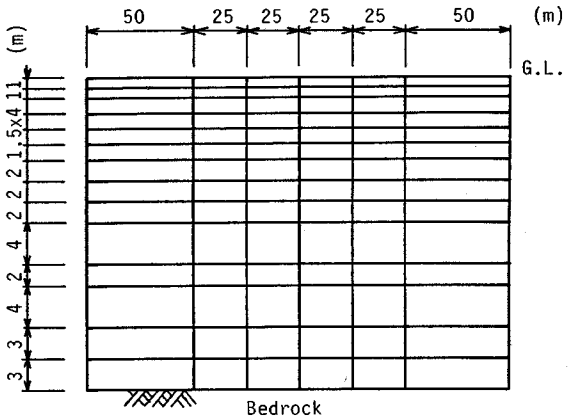

Fig. 2 Finite elements of the ground.

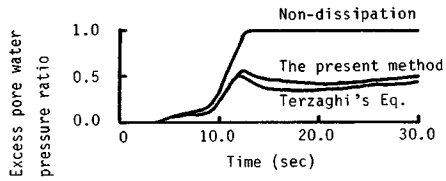

Fig. 3 Time histories of the excess pore water pressure.

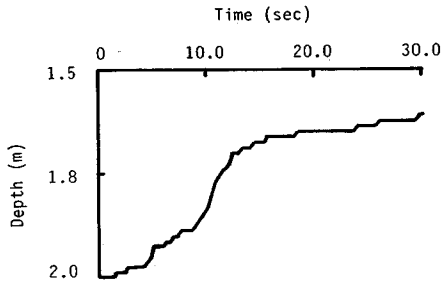

Fig. 4 Time history of the ground water level.

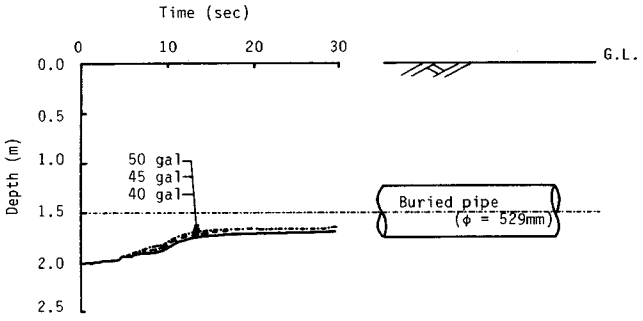

Fig. 5 Rise of the ground water level and location of the buried pipe (Model ground I).

pressure ratio increases to 1.0 in the method neglecting dissipation of the pore water pressure. It is about two times as much as the results considering the dissipation. Fig. 4 indicates the time history of the ground water level. Figs. 3 and 4 suggest that the ground water table rises when the excess pore water pressure at the 4th sand layer, located under the ground water table, rapidly increases. Fig. 5 shows the time history of the ground water level in relation to the location of the embedded pipeines in case of 40gal, 45gal and

Table 2 Dimensions of the pipeline.

Ductile cast iron pipe		
Outer diameter	(mm)	529
Thickness	(mm)	9.5
Young's modulus	(kgf/cm^2)	1.6×10^6
Length	(cm)	500
Specific gravity	(gf/cm^3)	7.15
Spring constant for rotation	($kgf \cdot cm/°$)	4.9×10^5
Spring constant for translation	(kgf/cm^2)	8500

($1gf/cm^3$ =9.8kN/m^3, $1kgf/cm^2$= 98kPa)

Table 3 Physical properties of model ground Ⅱ.

Depth (m)	Layer number	Initial shear modulus (kgf/cm^2)
1.0	1	60
2.0	2	60
3.5	3	100
5.0	4	300
6.5	5	700
8.0	6	1000

($1kgf/cm^2$ = 98kPa)

Other conditions are the same as in Table 1.

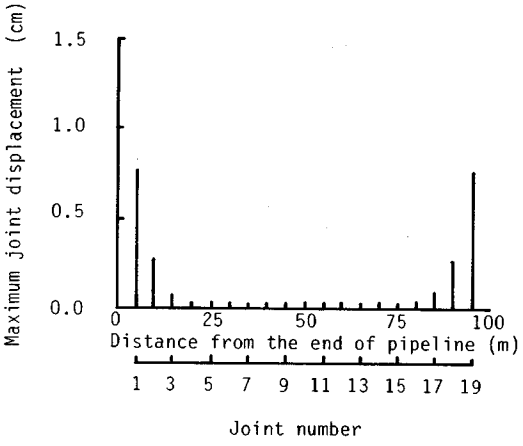

Fig. 6 Distribution of maximum joint displacement (Model ground Ⅰ).

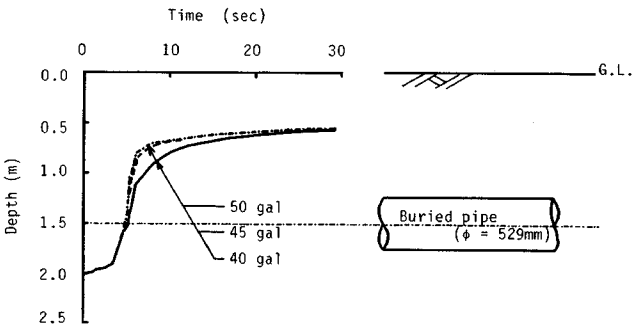

Fig. 7 Rise of the ground water level and location of the buried pipe (Model ground Ⅱ).

50gal maximum base motion acceleration. The surrounding soil is not saturated and does not liquefy after the rise of the ground water table in these examples. The maximum accelerations at the surface are 269gal, 285gal and 304gal in these cases, respectively. The large magnification of about six is explained in terms of no consideration of damping due to dissipating energy.

Fig. 6 shows the response of the buried pipelines for a maximum base motion acceleration of 45gal. The ductile iron pipelines with 529mm diameter consisting of 20 pipes connected by 19 corresponding joints are calculated. The two ends of a pipeline are assumed to be fixed to buildings. The burial depth is 1.5m. The pipeline is, therefore, buried at the 2nd layar in Fig. 2. The shaking direction is assumed to be parallel to the axis of the pipelines. Table 2 indicates the dimensions of the pipeline which is used in the calculations. Fig. 6 reveals that the joint displacement is large near the buildings and the maximum joint displacement is about 0.8cm. As this value is much lower than the allowable displacement of pull out at the joint, 5cm, the pipeline does not fail at the joints.

A sand deposit which is looser than that in the previous example shown in Table 3 is analyzed. This model corresponds to the ground whose SPT N-value at the surface ground is nearly 1. Fig. 7 indicates the time history of the ground water table in relation to the location of the buried pipelines. This figure reveals that the surrounding soil became saturated due to the rise of the ground water table. The maximum accelerations at the surface are 196gal, 222gal, 275gal in case of 40gal, 45gal, 50gal maximum base motion acceleration, respectively. The response of buried pipelines is shown in Figs. 8 and 9, for a maximum base motion acceleration of 45gal. These figures indicate the maximum joint displacement and the maximum displacement angle at joints, respectively. In this case, the buoyancy acting on the pipelines caused the

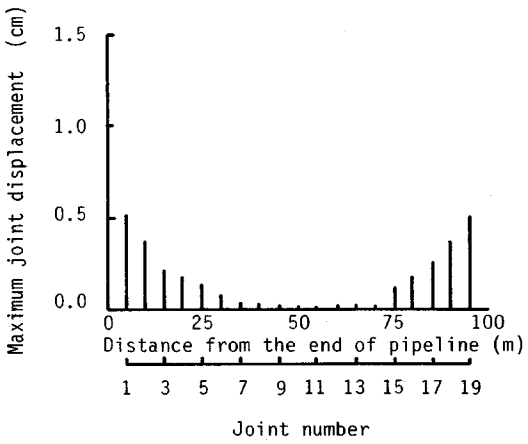

Fig. 8 Distribution of maximum joint displacement (Model ground Ⅱ).

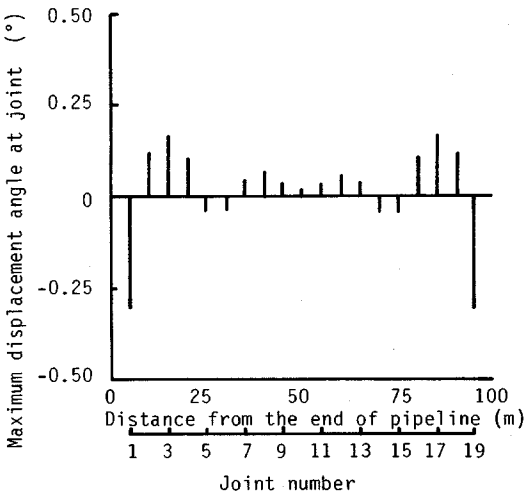

Fig. 9 Distribution of maximum displacement angle at joint (Model ground Ⅱ).

displacement angle at the joint because the surrounding soil was completely liquefied after the rise of the ground water table. This did not happen in the previous example and it was one of the characteristics of pipe behavior in the liquefied ground. Fig. 8 indicates the large joint displacements which were connected at their ends to a building. The maximum joint displacement was, however, only about 0.5mm. It was smaller than that in the previous example. This suggests that the higher the degree of liquefaction, the smaller the probability of the pipe's failure due to the ground vibration. On the other hand, it is important to consider the buoyancy effect as the excess pore water pressure becomes high. This means that the mechanism of pipe failure changes in the liquefaction process. Therefore, countermeasures corresponding to each mechanism had to be provided. Fig. 9 indicates that the displacement angle at joints is large near a building as a whole with a maximum value of 0.3°. The probability of joint failure is small in this case because the allowable displacement angle at a joint is 7°.

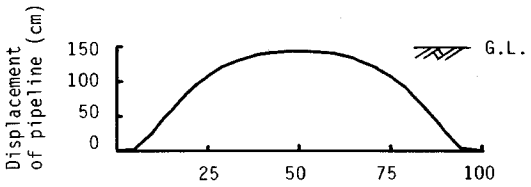

Fig. 10 Displacement of a pipeline.

According to Eq. (16), the soil spring constant of completely liquefied ground is 47 permill of the initial soil spring constant. It must be made clear how much the soil spring constant for completely liquefied ground is. It is, however, conceivable that the constant could be near to zero than that value. Fig. 10 shows the displacement of pipelines in completely liquefied ground where the soil spring constant is 3 permill of the initial value. The center of the pipeline almost floats to the surface of the ground. The maximum displacement angle at a joint is 2° and lower than the allowable value of 7°. The deformed pipeline as shown in this figure, however, will not be usable after an earthquake.

7. CONCLUDING REMARKS

The present paper proposed a hybrid procedure to analyze the behavior of buried pipelines in soil liquefaction process. Conclusions obtained from numerical examples are summarized as follows:

(1) The rise of the ground water table due to soil liquefaction can be properly evaluated by means of the method proposed in the present paper.

(2) The response of the pipelines can be investigated when the unsaturated sand layer around the pipelines liquefies, considering the rise of the ground water table and accumulation of excess pore water

pressure.

(3) It became evident from the numerical examples that the response characteristics of buried pipelines change in the liquefaction process. When the excess pore water pressure is low, the effect of the ground motion on the pipelines is predominant. The higher it is, the larger is the buoyancy effect.

(4) It is important to assess the soil spring constant more quantitatively in order to discuss the failure of the pipelines due to the buoyancy in complete liquefaction.

The failure of the pipelines due to the ground vibration could not be discussed in the numerical examples presented herein. It is explained in terms of the uniform conditions of a pipe oriented horizontally and parallel to the ground surface in these examples. A further study is needed from this point of view.

ACKNOWLEDGEMENT

The authors wish to acknowledge Professor T. Kobori for his kind advise throughout the present study. A part of expense of this study was defrayed by a Grant-in Aid for scientific research from the Ministry of Education, Science and Culture in Japan (No. 60750417). The calculation was performed by FACOM M-170F and FACOM M-360AP computers at the Kanazawa University Data Processing Center.

REFERENCES

1) Goto, K., Sato, A. and Akiba, M. : Investigation of Water Supply Installation Affected by the 1983 Mid-Japan Sea Earthquake, Journal of Japan Water Works Association, Vol. 54, No. 6, pp. 25~59, 1985 (in Japanese).
2) Kitaura, M. and Miyajima, M. : Quantitative Analyses on Damage to Buried Pipelines due to 1983 Middle Japan Sea Earthquake, Memoirs of the Faculty of Technology, Kanazawa University, Vol. 18, No. 2, pp. 57~65, 1985.
3) Finn, W. D. L., Lee, K. W. and Martin, G. R. : An Effective Stress Model for Liquefaction, Proc. of ASCE, Vol. 103, No. GT6, pp. 517~533, 1977.
4) Liou, C. P., Streeter, V. L. and Richart, F. E. : Numerical Model for Liquefaction, Proc. of ASCE, Vol. 106, No. GT6, pp. 589~606, 1977.
5) Koike, T. : Estimation of Buried Pipe Strains under Seismic Risk, Proc. of JSCE, No. 331, pp. 13~24, 1983 (in Japanese).
6) Takada, S., Takahashi, S. and Yamabe, Y. : Seismic Response of Buried Polyvinyl Chloride Pipeline, Journal of Japan Water Works Association, No. 547, pp. 27~39, 1980 (in Japanese).
7) Sato, H., Katsuki, S. and Ishikawa, N. : Elastic-Plastic Analysis of Plane Buried Pipelines under Forced Ground Deformation, Proc. of JSCE, No. 350, pp. 217~226, 1984 (in Japanese).
8) Kitaura, M., Miyajima, M. and Matsumura, Y. : Response Analysis of Buried Pipelines during soil Liquefaction, Proc. of the 17th JSCE Conference on Earthquake Engineering, pp. 303 ~306, 1983 (in Japanese).
9) Yoshikuni, H., Uno, H. and Yanagisawa, E. : Soil Mechanics(II), Gihodo-Shuppan, pp. 215~224, 1984 (in Japanese).
10) Brooks, R. H. and Corey, A. T. : Properties of Porous Media Affecting Fluid Flow, Proc. of ASCE, Vol. 92, No. IR2, pp. 61~88, 1966.
11) Martin, G. R., Finn, W. D. L. and Seed, H. B. : Fundamentals of Liquefaction under Cyclic Loading, Proc. of ASCE, Vol. 101, No. GT5, pp. 423~438, 1975.
12) Hardin, B. O. and Drnevich, V. P. : Shear Modulus and Damping in Soil : Design Equations and Curves, Proc. of ASCE, Vol. 98, No. SM7, pp. 667~691, 1972.
13) Drnevich, V. P. : Undrained Cyclic Shear of Saturated Sand, Proc. of ASCE, Vol. 98, No. SM7, pp. 807~825, 1972.
14) Toki, K. : Earthquake Resistance Analysis of Structures, Gihodo-Shuppan, pp. 77~80, 1981 (in Japanese).
15) Finn, W. D. L., Byrune, P. M. and Martin, G. R. : Seismic Response and Liquefaction of Sand, Proc. of ASCE, Vol. 102, No. GT8, pp. 841~856, 1976.
16) Nakamura, H. : A Modified Transfer Matrix Method with Improved Round off Errors, Proc. of JSCE, No. 289, pp. 43~53, 1979 (in Japanese).
17) Yoshida, T. and Uematsu, M. : Dynamic Behavior of a Pile in Liquefaction Sand, Proc. of the 5th Japan Earthquake Engineering Symposium-1978, pp. 657~663, 1978 (in Japanese).

(Received April 30 1986)